NMR Evidence for Dynamic Secondary Structure in Helices II and III of the 5S RNA of *Escherichia coli*†

Neocles B. Leontis‡ and Peter B. Moore*

Department of Chemistry, Yale University, New Haven, Connecticut 06511

Received December 3, 1985; Revised Manuscript Received March 4, 1986

ABSTRACT: A new ribonuclease A (RNase A) resistant fragment of the 5S ribonucleic acid (RNA) from *Escherichia coli* has been isolated and characterized. This fragment comprises helix III and most of helix II of the parent molecule, a part of the 5S RNA molecule for which several energetically equivalent secondary structures have been proposed [De Wachter, R., Chen, M.-W., & Vandenberghe, A. (1984) *Eur. J. Biochem. 143*, 175–182]. The imino proton spectrum of this fragment has been studied by nuclear magnetic resonance methods at 500 MHz. The data obtained are readily rationalized in terms of one of the structures proposed for this region of 5S RNA. They also suggest that upon heating, this structure is replaced by a second, different one, consistent with the view that the helix II–helix III region of 5S RNA is able to switch between alternative structures. Among the products of the nucleolytic digestion of 5S RNA is a species whose sequence indicates that RNase A can ligate RNA as well as hydrolyze it.

The 5S ribonucleic acid (RNA)[1] is the smallest of the ribosomal RNAs and as such has long been regarded as the system of choice for many kinds of investigations of rRNA structure and function. For several years, we have been studying 5S RNA and its complexes with ribosomal proteins by proton NMR, concentrating on the downfield spectrum (10–15 ppm downfield of DSS). The resonances which appear in that part of the proton spectrum of a nucleic acid come from imino protons involved in hydrogen bonding (Kearns & Shulman, 1974). Thus, if the downfield spectrum of an RNA can be interpreted, information about its secondary structure and dynamics can be obtained.

The sequence of the 5S RNA from *Escherichia coli* is shown in Figure 1a in the three-stemmed secondary structure proposed for it on the basis of sequence comparisons. Both the conformations proposed by De Wachter et al. (1982) for the helix II–helix III region are given in a slightly modified form which will be explained below. Because of its large size, progress in assigning the downfield spectrum of 5S RNA has depended on the isolation of smaller, more tractable fragments from it by limited nucleolytic digestion. Our previous studies have concentrated on helices I, IV, and V because of the availability of a fragment including that region of the molecule, bases 1–11 and 69–120. NMR work has also been reported by Chang et al. (1985) on nuclease-resistant fragments of wheat germ 5S RNA.

Below we report the isolation and characterization of a fragment of *E. coli* 5S RNA comprising most of the helix II–helix III portion of the molecule. The results of our initial analysis of the downfield spectrum of this fragment are reported and discussed in light of existing models for the secondary structure of this region of the molecule. Evidence for a magnesium-dependent, thermally induced conformational switch is presented and related to the behavior of intact 5S RNA.

Materials and Methods

5S RNA. The 5S RNA used for all experiments described below is the rrnB gene product obtained from the overproducing strain HB101/pKK5-1 (Brosius et al., 1984). Details of the methods used for overproduction and isolation of the 5S RNA from this strain have been described previously (Kime & Moore, 1983a). The rrnB gene product differs from the consensus *E. coli* sequence in that it has an A at position 12 rather than a C. The overproduced material also differs from normal, mature 5S RNA in having a few extra bases at both its 3′ and its 5′ ends (Kime et al., 1984).

Gel Electrophoresis. RNA and RNA–protein complexes were analyzed on "native" gels whose composition was 10% acrylamide, 0.5% bis(acrylamide), 0.08% TEMED, and 0.05% ammonium persulfate. The buffer (0.1 M KCl, 5 mM $MgCl_2$, and 50 mM Tris–borate, pH 7.8) was recirculated during electrophoresis, which was carried out at room temperature at 3 V/cm for 16 h. The oligonucleotide compositions of different RNA fractions were examined on urea-containing "denaturing" gels [12% acrylamide, 8 M urea, 0.5% bis(acrylamide), 0.08% TEMED, and 0.05% ammonium persulfate]. The buffer was 89 mM Tris–borate and 2.5 mM EDTA, pH 8.3. Gels were run at room temperature at 15 V/cm.

RNA Sequencing. Oligonucleotides isolated from denaturing gels were sequenced according to the method of Donnis-Keller et al. (1977) which provides positions for A's, G's, and pyrimidines. Since the primary structure of 5S RNA is already known, data of this kind were sufficient for this work. Most sequences were obtained by using oligonucleotides la-

† Supported by National Institutes of Health Grant GM32206. The Yale 490-MHz NMR spectrometer was supported by NIGMS Shared Instrumentation Program Grant GM 32243-02S1.

* Address correspondence to this author.

‡ Present address: Department of Chemistry, Bowling Green State University, Bowling Green, OH 43403. This work is from a dissertation submitted to the Graduate School of Yale University in partial fulfillment of requirements for the Ph.D. degree.

[1] Abbreviations: NMR, nuclear magnetic resonance; ADA, alternate delay accumulation; EDTA, disodium ethylenediaminetetraacetate; MES, 2-(*N*-morpholino)ethanesulfonic acid; NOE, nuclear Overhauser effect; RNA, ribonucleic acid; RNase, ribonuclease; SDS, sodium dodecyl sulfate; TEMED, *N,N,N′,N′*-tetramethylethylenediamine; DSS, 3-(trimethylsilyl)-1-propanesulfonate; Tris, tris(hydroxymethyl)aminomethane.

0006-2960/86/0425-3916$01.50/0

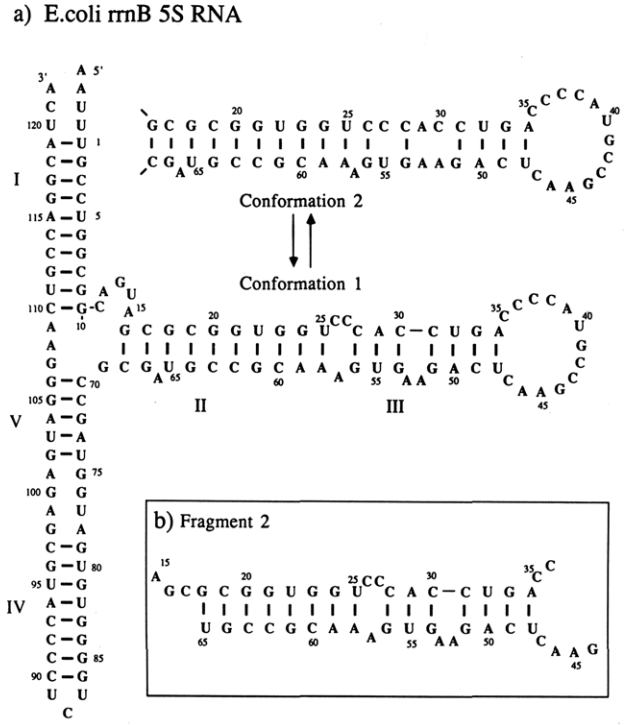

FIGURE 1: (a) Primary and secondary structure of *E. coli* rrnB 5S RNA showing two alternative conformations for the helix II–helix III region. (b) Strands 2 and 3 of fragment 2 in conformation 1.

beled at the 5′ end with T4 polynucleotide kinase. Polynucleotide kinase, T1 RNase, and U2 RNase were obtained from Bethesda Research Laboratories. RNase A was purchased from Sigma.

NMR Spectroscopy. All spectra reported below were obtained in the Fourier-transform mode on either the 500-MHz or the 490-MHz NMR spectrometers at the Yale University Chemical Instrumentation Center. Samples were dialyzed into buffers containing 105% of the stated concentrations of supporting electrolytes. Following dialysis, 5% D_2O was added to the samples for the spectrometer lock. Samples were concentrated by ultrafiltration using Centricons (Amicon). Dioxane was added at 2 mM concentration to each sample for chemical shift referencing and was assumed to have a chemical shift of 3.741 ppm relative to the methyl resonance of 3-(trimethylsilyl)-1-propanesulfonic acid at all temperatures. The stability of the temperature control system for day to day or during long runs was monitored by following the chemical shift of the water proton resonance, which is temperature dependent.

Spectra of the exchangeable imino protons were taken by using the twin pulse method for avoiding excitation of the water solvent resonance (Kime & Moore, 1983a) in combination with alternate delay accumulation (ADA) (Roth et al., 1980) to overcome computer word length limitations. Spectra were taken in 16K or 8K blocks with a spectral width of 12 000–15 000 Hz and the offset at 15 ppm.

NOEs between hydrogen-bonded imino protons were obtained by the one-dimensional difference method. On-resonance spectra, in which an imino resonance was preirradiated by using the decoupling channel, and off-resonance spectra used for differencing were collected an interleaved manner. Resonances were typically preirradiated for 0.3 s at a decoupler power level adjusted to give 50–75% saturation. The free induction decay was subjected to Lorentzian to Gaussian multiplication prior to Fourier transformation in order to improve resolution of NOEs or simple exponential multiplication

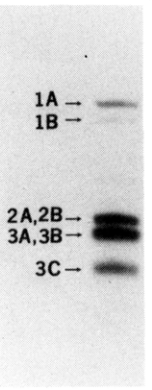

FIGURE 2: Component strands of fragment 2 preparation run on urea denaturing gel (see Materials and Methods). The numbering system for the strands is given.

(1–5 Hz) for noise suppression. ADA was not used in recording the NOEs from AU resonances to upfield aromatic protons.

RESULTS

Conditions for Production of a Fragment Containing Helices II and III of 5S RNA. In the course of optimizing conditions for producing "fragment 1" (bases 1–11, 69–120) by RNase A digestion of intact 5S RNA, it was noticed that a second, smaller oligonucleotide fragment was appearing. Conditions for obtaining the latter product in good yield are as follows. Intact 5S RNA is dissolved in 0.1 M KCl, 10 mM magnesium acetate, and 50 mM Tris–boric acid, pH 7.8, at a concentration of 20 A_{260nm}/mL. RNase A is added to a final concentration of 1.1 μg/mL and the mixture incubated at 273 K. Digestion is stopped after 45 min by the addition of 1% SDS followed by phenol extraction. Fragment 2 may be separated from fragment 1 and other digestion products on Sephadex G-75 at 310 K in 0.1 M NaCl, 5 mM magnesium acetate, and 10 mM MES (pH 6.0).

Chemical Characterization of Fragment 2. Fragment 2 runs on native gels as a broad band substantially faster than fragment 1; it does not seem to be as homogeneous as fragment 1 by this criterion (data not shown). On denaturing gels, fragment 2 displays a complex oligonucleotide composition (Figure 2). In some samples, the bands labeled 2A and 2B and 3A and 3B in Figure 2 each resolve into two bands on high-resolution denaturing gels. The oligonucleotides numbered in Figure 2 were eluted from high-resolution gels and sequenced. The RNA which was eluted from band 3A did not differ from 3B in sequence. Neither did band 2A differ from 2B. There is some indication that the doubling in each case may be due to formation of 2′,3′-cyclic phosphates on the 3′ ends of strands 2 and 3. Strand 3A,3B extends from A15 to the pyrimidine tract starting at C35 (see Figure 1). There is heterogeneity at the 3′terminus of 3A,3B; it terminates at C35 or C36. Strand 3C begins at G18 and like 3A,3B ends at C35 or C36. Strand 2A,2B begins at G44 and ends at U65. A66, the "bulged A" in helix II (Peattie et al., 1981), is thus missing in fragment 2 along with G67 and C68 which are involved in base pairs in the standard model. The residues constituting strands 2 and 3 of fragment 2 are shown in Figure 1b.

Strands 1A and 1B have surprising sequences. What we anticipated was that 1A and 1B would start at A15 or G18 and continue through the loop (at G41) to U65. What was found is that, although A15 and G18 are 5′ termini for 1A and 1B and U65 is the 3′ terminus, there is only one residue,

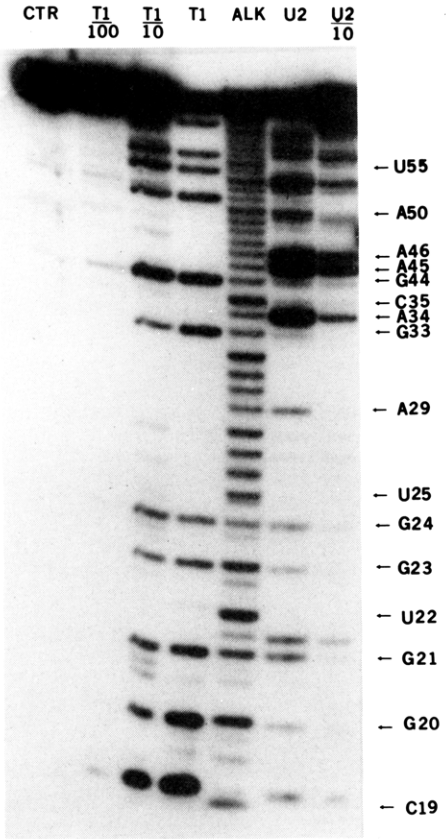

FIGURE 3: Sequencing gel of strand 1 showing ligation by RNase A of the pyrimidine at position 35 to G44. CTR, control lane; ALK, ladder produced by alkaline digestion; T1, digestion with G-specific RNase T1; T1/10 and T1/100, 1:10 and 1:100 dilutions in amount of T1; U2, digestion with A-specific RNase U2; U2/10, 1:10 dilution in amount of U2. Note that some length heterogeneity is evident in the alkaline ladder. Some cutting by U2 is observed at G's as well as A's.

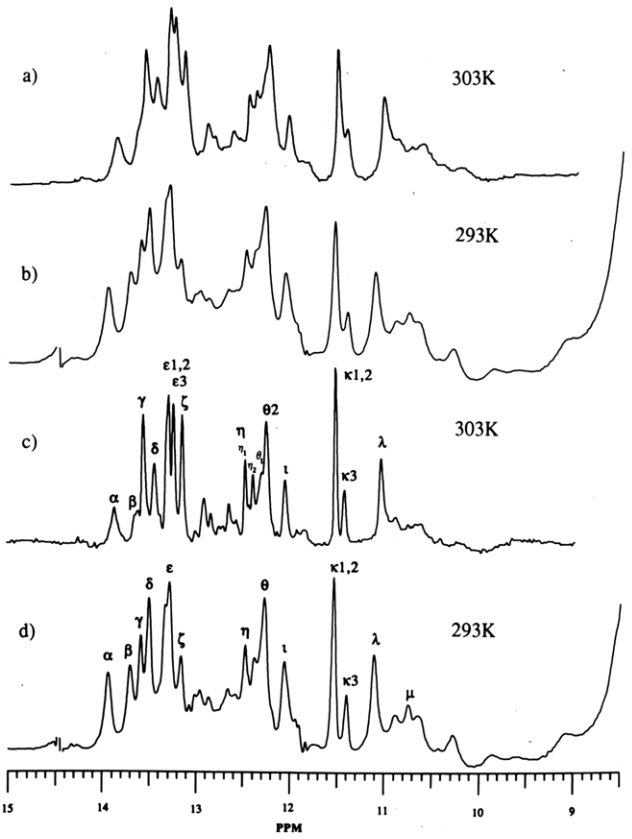

FIGURE 4: Spectra of fragment 2 (about 4 mM) in 0.1 mM $MgCl_2$, 0.1 M KCl, and 2 mM MES at pH 5.5 taken at (a) 303 and (b) 293 K and shown resolution enhanced, with resonances labeled in (c) and (d).

a pyrimidine, between A34 and G44. Sequencing data which demonstrate this fact are shown in Figure 3. The possibility that the plasmid being used for producing native 5S RNA had suffered a deletion was ruled out by sequencing the G41 region of its intact 5S product; it is normal. Thus, it is clear that during RNase A digestion, residues 36–43 are excised from the 5S molecule and the loop religated. This religated form of fragment 2 accounts for about 5% of the molecules in a typical preparation.

Protein Binding. It is easy to demonstrate the binding of ribosomal proteins L25 and L18 to 5S RNA electrophoretically on native gels and to show that L25 binds to fragment 1 but that L18 does not [e.g., see Douthwaite et al. (1979)]. Protein binding reduces the electrophoretic mobility of an RNA. By this criterion, fragment 2 does not bind L18 even though it includes most of the L18 binding site in 5S RNA (Douthwaite et al., 1982). All component strands of fragment 2 end at U65. Since A66 contributes significantly to the interaction of 5S RNA with L18 (Peattie et al., 1981; Christiansen et al., 1985), the failure of fragment 2 to bind to L18 is perhaps understandable. It is possible, however, that at the high concentrations used in NMR samples, interaction between fragment 2 and L18 might be observable.

Downfield Spectrum of Fragment 2. The downfield spectrum of fragment 2 in 5 mM MES, pH 5.5, 0.1 mM $MgCl_2$, and 100 mM KCl is shown in Figure 4 at (a) 303 K and (b) 293 K. Figures 4c,d shows the same spectra resolution-enhanced to facilitate identification of resonances. The fragment 2 resonances are given Greek letter designations to distinguish them from the Roman letter designations assigned to fragment 1 resonances previously (Kime & Moore, 1983a). As will become clear below, many of the resonances in the fragment 2 spectrum represent the contributions of several different imino protons; the different components of a given resonance in Figure 4 will be designated with numerals.

A striking aspect of the spectrum of fragment 2 under these conditions is the sensitivity of resonances α, β, and ι to changes in temperature. When the temperature is raised from 293 to 303 K, α and β broaden, lose intensity, and shift upfield, while ι also loses intensity. On the other hand, ζ dramatically sharpens and may gain intensity. The resolution improves on raising the temperature, in part from the decreasing viscosity of the solution, but also because of minor chemical shift changes on the part of resonances δ, $\epsilon 3$, $\eta 2$, and $\theta 2$.

The spectra in Figure 4 include resonances which have low intensity or are particularly broad. A number of these occur between 12.5 and 13.0 ppm, and upfield of resonance λ. These resonances are also sensitive to temperature. Resonances $\eta 2$ and $\kappa 3$ are present in less than stoichiometric intensity under all conditions. A very broad resonance appears at 14.6 ppm at temperatures below 288 K, which narrows as the temperature is lowered from 283 to 276 K but does not reach full intensity (data not shown).

Nuclear Overhauser Experiments on Fragment 2: (*A*) *Tentative Assignments for Helix II Resonances.* As first demonstrated by Redfield and his colleagues (Johnston & Redfield, 1977, 1981; Sanchez et al., 1980; Roy & Redfield, 1981), nuclear Overhauser experiments are a powerful aid in assigning downfield spectra of nucleic acids. In general, only imino protons in base pairs which are immediate neighbors will show mutual NOEs. One can identify the resonances coming from successive base pairs in a helical RNA or DNA

Table I: Summary of NOEs Observed in Fragment 2

resonance	NOEs to	comments	base pair type
α	β	upfield NOE 7.53 ppm	AU
β	α	weak NOE 7.53 ppm	GC
γ	ζ	upfield NOE 7.37 ppm	AU
δ	$\theta 1$	upfield NOE 6.63 ppm	AU
$\epsilon 1,2$	κ,λ		GC
$\epsilon 3$	$\theta 2$		GC
ζ	γ		GC
$\eta 1,2$	none observed		
$\theta 1$	δ	upfield NOE 7.51 ppm	GA
$\theta 2$	$\epsilon 3$		GC
ι	none observed		
$\kappa 1,\kappa 3$	none observed		
$\kappa 2$	λ, $\epsilon 1,2$	λ NOE very strong	GU
λ	κ, $\epsilon 1,2$	κ NOE very strong	GU
μ	none observed		

by following NOE connectivities in the imino region. Moreover, AU's give strong intra-base-pair NOEs, due to the proximity of the UN3 imino proton to the AH2 proton, which resonates in the aromatic region, whereas GC's have no such aromatic correlate. On the other hand, GU base pairs, which are fairly common in RNA molecules, exhibit strong intra-base-pair NOEs between their GN1 and UN3 imino protons. Thus, both helical connectivities and base pair identities can be inferred from NOE data [e.g., see Hare & Reid (1982a,b) and Roy et al. (1982)].

NOE experiments have been done on all the resonances in the downfield spectrum of fragment 2, many of them under a variety of conditions to take advantage of the fact that the chemical shifts of many of the resonances in this spectrum are perturbed by modest changes in temperature or Mg^{2+} concentration. The results are summarized in Table I.

In order to organize the data, it is useful to examine some secondary structure models which have been proposed for helix II and helix III, the region of 5S RNA from which fragment 2 is derived. It has long been recognized that there is no unique "best" secondary structure for this molecule. Figure 1 shows the two alternative conformations proposed by De Wachter et al. (1982), slightly modified in that G24 is shown paired with A59, and U25 is paired with A58 for reasons which will be explained shortly. It will be noted that both forms of the structure include a GU (U22-G61) flanked by GC's. It is notable, therefore, that the most conspicuous NOE in the whole spectrum is the one which relates $\kappa 2$, the most prominent κ resonance, with λ. The strength of the NOE between $\kappa 2$ and λ (data not shown) and their upfield chemical shifts indicate that these two resonances arise from a GU base pair. $\kappa 2$ and λ both give NOEs to ϵ, and at 306 K, where $\epsilon 3$ can be adequately resolved from $\epsilon 1$ and $\epsilon 2$, it becomes clear that $\epsilon 1$ and $\epsilon 2$, the two more downfield components, relate to $\kappa 2$ and λ. Both $\epsilon 1$ and $\epsilon 2$ give NOEs back to $\kappa 2$ and λ but do not have aromatic NOEs. Therefore, it is likely that $\kappa 2$, λ, $\epsilon 1$, and $\epsilon 2$ represent U22-G61 and its two flanking GC's, G21-C62 and G23-C60. Which of the two GC's belongs to which ϵ resonance cannot be determined.

There is no NOE evidence for a second GU base pair in the spectrum to account for G18-U65 in Figure 1. Given that Watson–Crick base pairs at helix termini are often difficult to observe due to exchange broadening [e.g., see Chou et al. (1984)] and that GU's are believed to be no stronger than AU Watson–Crick pairs (Romaniuk et al., 1979), the absence of NOE evidence for another GU is not surprising.

Among the remaining NOEs observed in fragment 2, there is a mutual effect involving the upfield components of both ϵ and θ, namely, $\epsilon 3$ and $\theta 2$. Neither has an aromatic correlate

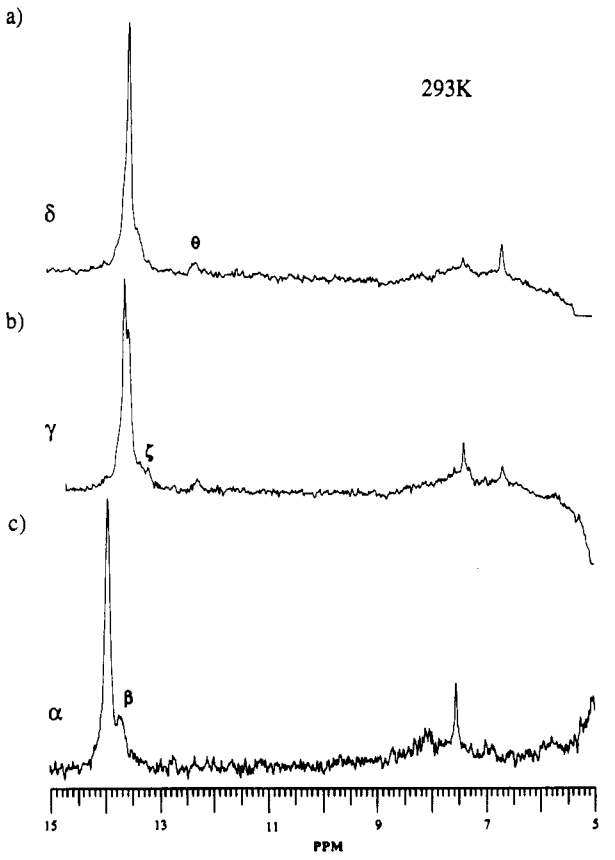

FIGURE 5: NOEs elicited by irradiation at (a) resonance δ, (b) resonance γ, and (c) resonance α, showing upfield aromatic NOEs at 6.63, 7.37, and 7.53 ppm, respectively. Data were collected without ADA and were subjected to 5-Hz line broadening.

and so are likely to represent a (GC)-(GC) sequence. The most likely placement for this pair of resonances is C19-G64 and G20-C63. Again, it is unclear which way around the two resonances should be assigned.

(*B*) *Helix III.* De Wachter et al. (1982) have proposed two different structures for *E. coli* 5S RNA in the helix III region. As drawn in Figure 1, both structures include an AU-AG sequence of base pairs (G24-A59 and U25-A58). The reason we have added these base pairs is that without them the helix II-helix III region contains no more than two internal AU base pairs, and the NMR data clearly show that there are three. Three resonances in the spectrum have both the chemical shifts and aromatic NOEs expected for AU base pairs, α, γ, and δ. NOE difference spectra obtained at 293 K for these resonances are shown in Figure 5. These spectra were taken without ADA, which significantly suppresses intensities in the aromatic region. It should be noted that the aromatic correlate of resonance δ occurs at 6.63 ppm, upfield of the normal range for AH2 protons.

α and β give mutual NOEs as do γ and ζ, suggesting two AU-GC sequences. The third AU, δ, gives an NOE to $\theta 1$, and $\theta 1$ itself has an aromatic correlate at 7.50 ppm. This is illustrated in Figure 6. This spectrum was obtained at 288 K with ADA (which attenuates the aromatic region by a factor of 2 or 3) in a sample prepared in 5 mM Mg^{2+}. The upfield NOE from the θ region has not been observed at higher temperature or lower Mg^{2+} concentration. There is no (AU)-(AU) sequence in fragment 2. There is, however, the possibility of forming an AU at U25-A58 next to an AG, G24-A59. This suggests that δ is U25-A58 and $\theta 1$ the AG base pair in question, as shown in Figure 1. This AU-AG juxtaposition is peculiar to the *E. coli* sequence; base pairing at these

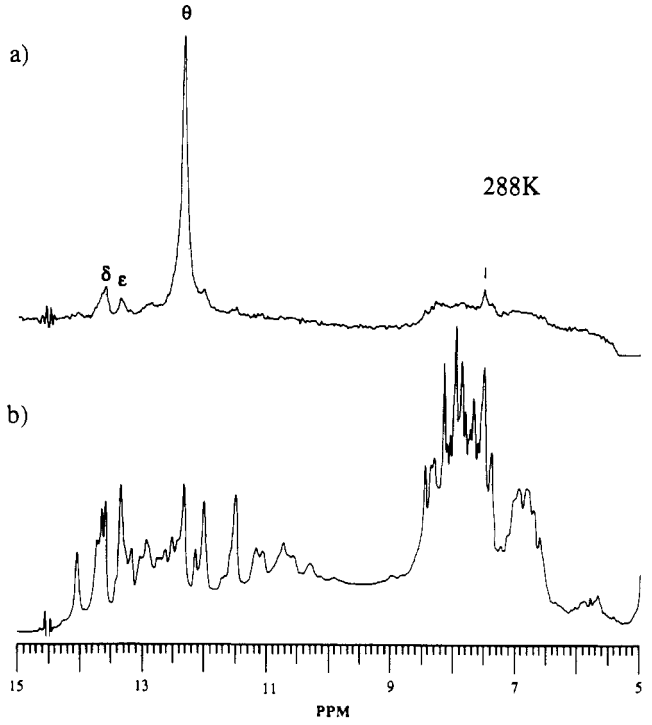

FIGURE 6: NOEs elicited by irradiation at resonance θ at 288 K in 5 mM $MgCl_2$, 0.1 M KCl, and 5 mM MES at pH 6.0. (a) Difference NOE spectrum showing upfield NOE to aromatic resonance at 7.51 ppm (arrow) and NOEs to δ and ϵ region. FIDs subjected to 5-Hz line broadening. (b) Reference spectrum, shown resolution enhanced. Spectra were collected with ADA.

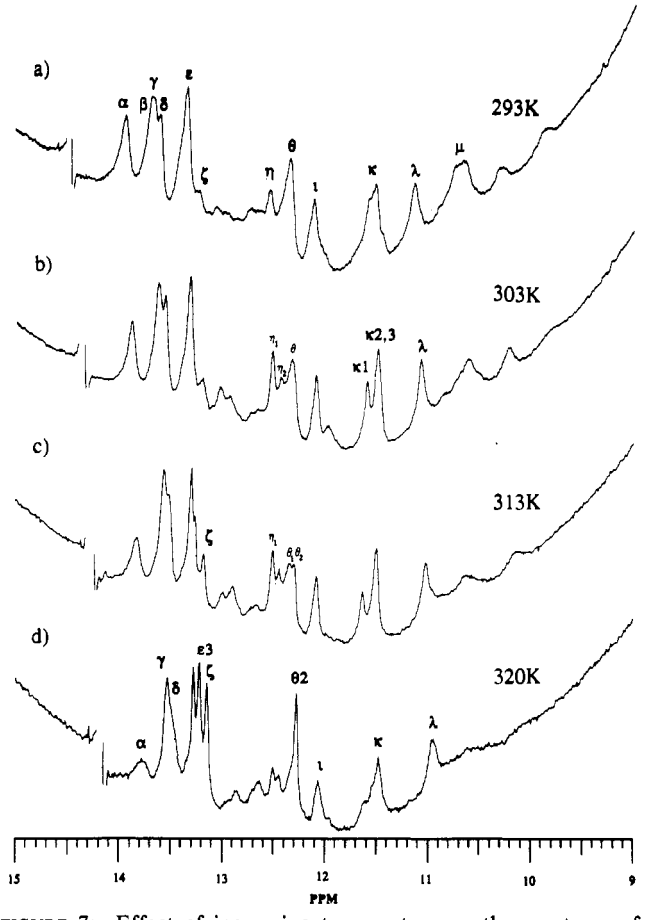

FIGURE 7: Effect of increasing temperature on the spectrum of fragment 2 in high magnesium (about 5 mM $MgCl_2$, 0.1 M KCl, and 2 mM MES at pH 5.5). Spectra are shown without resolution enhancement or base-line correction.

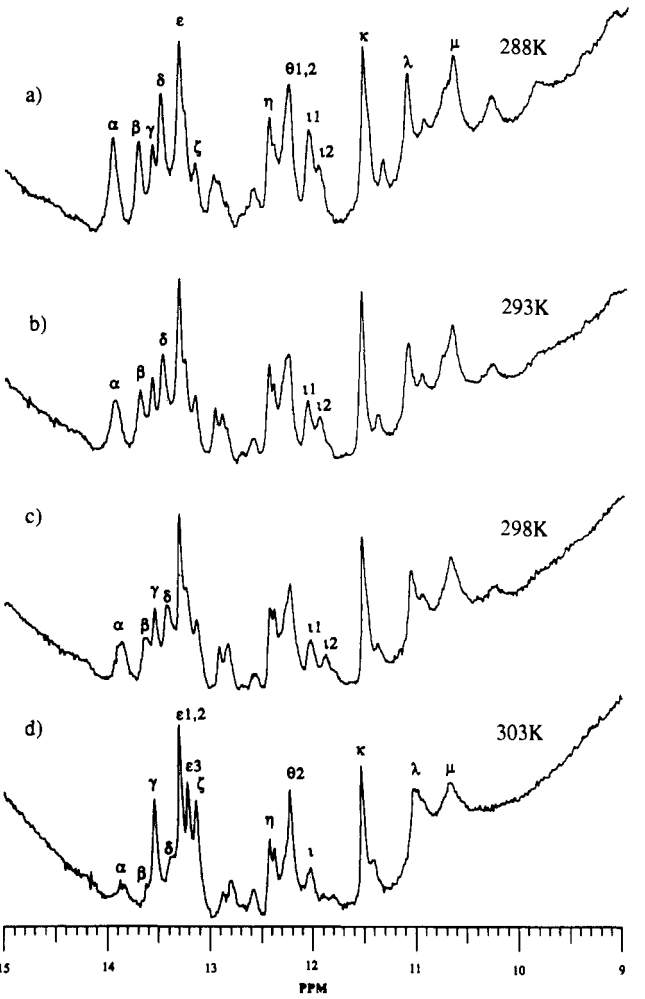

FIGURE 8: Effect of increasing temperature on the spectrum of fragment 2 in low magnesium (30 μM $MgCl_2$, 0.1 M KCl, and 2 mM MES at pH 5.5). Spectra are shown without resolution enhancement or base-line correction.

positions is not included in universal models for 5S RNA (Delihas et al., 1984). By elimination, α, β and γ, ζ represent the two internal AU's in helix III, and one of the two GC's which presumably flank each of them. It follows that the molecule must be in conformation 1 because in conformation 2 only two internal AU base pairs are formed.

Environmental Effects on Fragment 2. In comparison with fragment 1, the spectrum of fragment 2 is remarkably sensitive to environmental conditions. Relatively modest changes in Mg^{2+} concentration and temperature lead to substantial spectral changes, as already shown in Figure 4. The behavior of the molecule has been examined at a variety of temperatures and Mg^{2+} concentrations (but a constant ionic strength, 0.1 M KCl) in an effort to understand what is going on.

Figure 7 shows spectra for fragment 2 taken in high Mg^{2+} concentration (pH 5.5, about 5 mM $MgCl_2$ and 100 mM KCl) at progressively higher temperatures from 293 to 320 K. As in the case at 0.1 mM Mg^{2+} (Figure 4), the most conspicuous change is the selective melting of resonances α and ι and the dramatic intensity increase of resonance ζ, which is connected by NOE to γ, and of resonances $\eta 1$ and $\eta 2$. In 5 mM Mg^{2+}, β shifts upfield and cannot be resolved from γ. Unlike the situation at low Mg^{2+}, concentration, resonances δ and $\theta 1$ resist melting even at 313 K, where α and ι are significantly broadened.

Reducing the Mg^{2+} concentration has the effect of reducing the temperatures over which the selective melting of α, β, and

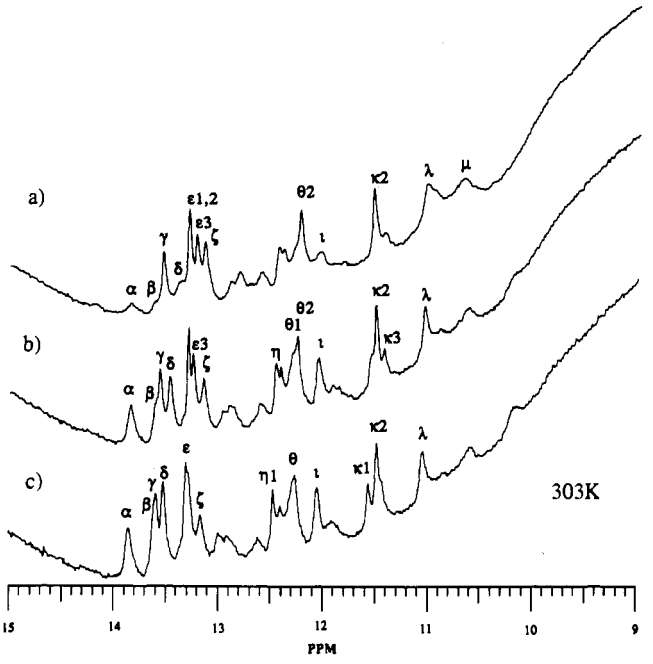

FIGURE 9: Titration of fragment 2 spectrum with Mg^{2+} at 303 K in 0.1 M KCl and 5 mM MES at pH 5.5. (a) 30 μM $MgCl_2$; (b) spectrum similar to that observed in 0.1–0.5 mM Mg^{2+}; (c) spectrum similar to that observed in 5 mM Mg^{2+}. Spectra were not resolution enhanced or base-line corrected.

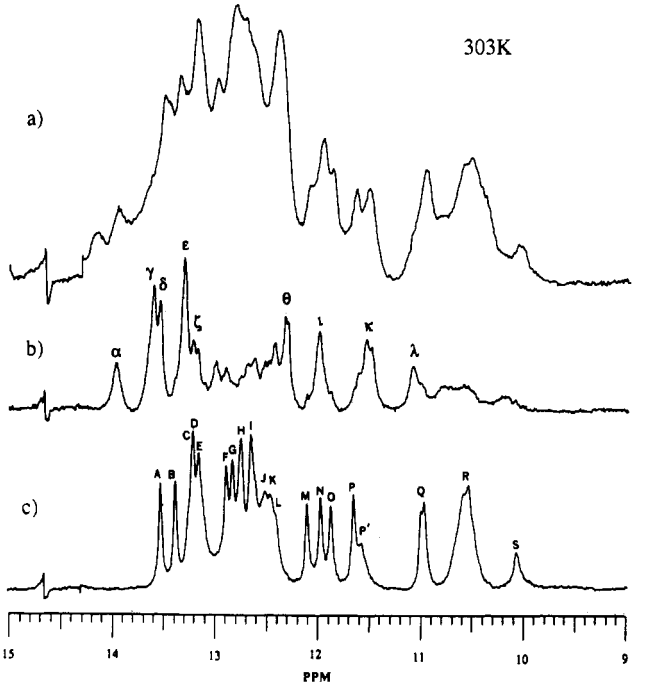

FIGURE 10: Comparison of spectra of whole 5S RNA and fragments 1 and 2 taken under identical conditions: 303 K in 5 mM $MgCl_2$, 0.1 M KCl, and 5 mM MES at pH 6.0. (a) Intact rrnB 5S RNA; (b) fragment 2; (c) fragment 1, intact in the loop at bases 87–90. Spectra were subjected to 1–3-Hz line broadening and base-line correction.

ι occurs. Spectra taken at 0.030 mM Mg^{2+} are shown in Figure 8 covering the temperature range 288 to 303 K. It is apparent that at very low Mg^{2+} concentration the melting of resonances α, β, and ι is almost complete by 303 K, while the melting of resonances upfield of μ is totally complete. Moreover, the range of temperature over which these changes occur is narrowed by the reduction in Mg^{2+} concentration. The resonances of fragment 2 are present in full intensity in the spectrum taken at 288 K, and the sensitive resonances are gone at 303 K. Lowering the Mg^{2+} concentration also makes resonances δ and $\theta 1$ more sensitive to temperature. Both resonances are strongly exchange broadened by 303 K. This is clear in the case of δ, which appears at 303 K as a shoulder to the ϵ resonances, but is harder to discern in the case of $\theta 1$, which coincides with $\theta 2$. It should also be noted that in low Mg^{2+} (and below 288 K in high Mg^{2+}) resonance ι splits into two resonances.

The partial melts shown in Figures 7 and 8 are fully reversible. By contrast, when the divalent ion concentration is reduced to zero by dialysis against EDTA solution at room temperature, most of the downfield resonances in the fragment 2 spectrum disappear, and the spectrum is not restored to normal by readdition of Mg^{2+}. The changes seen in the absence of Mg^{2+} suggest that the two strands of the molecule separate under these conditions. Intrastrand hairpin loop formation in the 5′ strand of fragment 2 (A15-C35) could account for the few strong resonances which remain in the imino spectrum. The strands do not appear to dissociate below 278 K, however. Samples which were first dialyzed exhaustively against EDTA at 278 K and then returned to Mg^{2+}-containing buffer exhibited normal imino spectra.

The effects produced by reducing the Mg^{2+} concentration to 0.03 mM are also fully reversible. The 0.03 mM Mg^{2+} spectrum at 303 K can be converted into a high Mg^{2+} spectrum at 303 K by direct addition of Mg^{2+}. Figure 9 shows the effect of gradual restoration of Mg^{2+} to the sample prepared at 0.03 mM Mg^{2+}. Spectrum 9b is comparable to those of samples prepared at 0.1–0.5 mM Mg^{2+}, while spectrum 9c is typical of samples prepared in 5 mM Mg^{2+}. The effect of adding small amounts of Mg^{2+} is dramatic. The spectrum is much less affected by changes in monovalent cation concentration (data not shown). Decreasing the Mg^{2+} concentration also has the effect of improving the resolution of fragment 2 spectra on account on a general reduction in line width and certain fortuitous chemical shift changes. At low Mg^{2+} concentration, β, γ, and δ are resolvable. Likewise, $\epsilon 3$ can be resolved from $\epsilon 1$ and $\epsilon 2$, and $\theta 1$ can be distinguished from $\theta 2$.

These results can be summarized as follows. First, resonances $\epsilon 1$, $\epsilon 2$, $\kappa 2$, and λ, as well as $\epsilon 3$ and $\theta 2$, all resist perturbation, suggesting that the core of helix II is reasonably stable. Likewise, γ and ζ in helix III, resonances connected to each other by NOE, resist melting. Second, α and β, and δ and $\theta 1$, pairs of resonances connected to each other by NOE, are particularly sensitive to temperature and divalent cation concentration. Resonances which come from the same part of the structure behave alike. Third, when temperature increases, not only do some resonances disappear, suggesting the expected melting of structure, but others gain intensity, a fact which points to the formation of alternative structures.

Comparison of the Spectra of Fragment 1, Fragment 2, and Whole 5S RNA. The spectra of whole 5S RNA, fragment 1, and fragment 2 are compared in Figure 10. Spectra were taken in 100 mM KCl, 5 mM $MgCl_2$, and 5 mM MES, pH 6.0 at 308 K. Fragment 2 supplies many of the features of the spectrum of the native molecule which are not found in fragment 1. Fragment 2 clearly is the source of the resonance which is present in whole 5S RNA but not in fragment 1 at the chemical shift of α. $^{15}N/^{1}H$ chemical shift correlation experiments done on intact 5S RNA indicate that this resonance is a UN3 imino proton resonance, consistent with the assignment of α to an AU base pair in fragment 2 (A. G. Redfield, M. Jarema, and P. B. Moore, unpublished results). We have examined the spectrum of whole rrnB 5S RNA at 0.3 mM Mg^{2+} (pH 7.2, 100 mM KCl) for evidence of tem-

perature-sensitive resonances. The most striking effect is the early melting of the resonance corresponding in chemical shift to α in fragment 2. The resonance is present in full intensity at 283 K but melts out completely by 298 K in 0.3 mM Mg^{2+}. By contrast, α does not melt out until over 308 K at this level of Mg^{2+} in fragment 2.

Resonance ι in fragment 2 adds to the intensity of resonance N in fragment 1 to give the 1:2:1 appearance of the M,N,O region of native 5S RNA. κ and λ correspond to the peak just upfield of P and the downfield shoulder of Q, in the 5S RNA spectrum, respectively. These features are also absent in the fragment 1 spectrum. The θ resonances account for the intensity seen in the intact 5S spectrum at 12.3 ppm where there is no intensity in fragment 1. These observations indicate that the helix II-III sequences in intact 5S RNA have a conformation similar to the one they assume in fragment 2. It is likely that in 1–5 mM Mg^{2+} at room temperature, intact 5S RNA is in conformation 1.

Discussion

Primary Structure of Fragment 2. In general, the termini of the component strands of fragment 2 are consistent with the results of Douthwaite and Garrett (1981), who determined the primary and secondary cleavage sites in *E. coli* 5S RNA for several ribonucleases, including RNase A. The sole exception is strand 1. In this molecule, the loop from C36 to C43 has been removed; all that remains are one or two pyrimidines. We are not aware of other reports of RNase A acting as a ligating enzyme, yet this seems to be what has taken place here.

Secondary Structure of Fragment 2. It is clear that there is insufficient NOE data available in the fragment 2 spectrum to allow a priori deduction of its secondary structure. Nevertheless, the NOE data and the behavior of the imino spectrum under environmental perturbations can be understood in terms of the secondary structure models generally accepted for this part of 5S RNA. The fact that three AU's are observed in the spectrum at moderate temperatures in the presence of Mg^{2+} is clear evidence that the native structure is conformation 1 (Figure 1). The AU resonance, δ, is assigned to U25-A58 on the basis of its NOE to $\theta 1$, which appears to arise from a GA base pair. The assignment of the other two AU's, α and γ, is ambiguous given the paucity of NOEs and the fact that both remaining AU's in structure 1 have two GC neighbors. Chemical shifts for the base pairs in conformation 1 were calculated by using the ring current shift rules derived for regular RNA helices, making no correction for bulged bases or nonstandard base pairs (Robillard, 1977; Kearns, 1976). Table II summarizes the chemical shifts calculated for fragment 2 by two different prediction schemes and compares them with our current assignments. The ambiguities surrounding the assignment of resonances α and β, γ and ζ, and $\epsilon 3$ and $\theta 2$ can be resolved in a tentative manner by appeal to these calculations. Thus, for example, they suggest that α should be assigned to the internal A29-U55 and γ to U32-A50.

The calculations also predict that the terminal base pair, A34-U48, of helix 3 should appear downfield of α. At low temperature, a broad resonance is observed below 14 ppm in the fragment 2 spectrum, while a thermally stable resonance is observed in whole 5S at RNA at 14.17 ppm (see Figure 10). These resonances may well correspond to A34-U48. The loop region in intact 5S RNA is known from nuclease sensitivity studies to be highly structured (Douthwaite & Garrett, 1981). It would not be surprising if this proton were protected from solvent exchange in the whole molecule but much less well protected in fragment 2.

Table II: Calculated and Observed Chemical Shifts (in ppm) of Fragment 2 Resonances and Proposed Assignment of Resonances

fragment 2	calculated A-RNA[a]	A′-RNA[b]	observed[c]	assigned resonance(s)
CGA-5′				
65-U-G				
G-C	13.0	12.8	12.3 or 13.3	$\epsilon 3$ (13.3)
C-G-20	12.7	12.2	12.3 or 13.3	$\theta 2$ (12.3)
C-G	13.4	13.25	13.3	$\epsilon 1$ or $\epsilon 2$
G-U			11.5/11.1	$\kappa 2/\lambda$
60-C-G	12.6	12.2	13.3	$\epsilon 1$ or $\epsilon 2$
A-G			12.3	$\theta 1$
A-U-25	13.6	13.2	13.5	δ
A C				
| C				
G C	12.1	11.5	13.7 or 13.15	ι? (12.06)
55-U-A	13.9	13.8	13.9 or 13.6	α (13.9)
A-G-C-30	13.3	13.4	13.7 or 13.15	β (13.7)
A-G-C	13.0	12.8	13.7 or 13.15	ζ (13.15)
50-A-U	13.65	13.3	13.9 or 13.6	γ (13.6)
C-G	12.15	11.5	13.7 or 13.15	$\kappa 1$? (11.6)
U-A	14.16	14.2		
C C-35				
C				
A				
G				

[a] Prediction method was from Robillard (1977). [b] Prediction method was from Kearns (1976). [c] Chemical shifts observed at 293 K in 0.1 mM $MgCl_2$, 0.1 M KCl, and 5 mM MES (pH 5.5). The chemical shifts given in the observed column correspond to all the resonances consistent with the NOE data, given that U22-G61 and U25-A58 are assigned to κ/λ and δ, respectively, and that resonances α and γ correspond to A29-U55 and U32-A50 or vice versa. The assignments given in the assigned resonances column are those most consistent with both the NOE data and the calculated chemical shifts.

Although no assignments are possible for G56-C28 or for C49-G33, it is notable that upfield chemical shifts are predicted for these base pairs and that in fact two upfield GC resonances are present in the spectrum with unit intensity, ι and $\kappa 1$. It is plausible to associate ι with G56-C28/C27 because it shares the thermal sensitivity of resonances α and β, which are assigned to the neighboring base pairs.

Table II also points out some of the difficulties with the assignment scheme we propose. The first, and most obvious, problem is the lack of NOE continuity in the helical regions. In helix II, this derives largely from the coincidental overlap of several key resonances, namely, $\epsilon 1$, $\epsilon 2$, $\epsilon 3$, $\theta 1$, and $\theta 2$. Conditions have not been found where these resonances are adequately resolved. Consequently, the strong NOE observed between $\epsilon 3$ and $\theta 2$ makes it difficult to confirm or deny the existence of the expected NOEs between $\epsilon 1$ or $\epsilon 2$ and $\theta 1$ on one side of helix II and $\theta 2$ on the other side of the helix. Similarly, a β to ζ NOE would be much appreciated to connect the center of helix III, as would contributions from the AU's α and γ onto the GC base pairs which flank them on the outside of helix III. While the absence of some of these "expected" NOEs can be rationalized by appeal to bulged bases and base pairing irregularities, their absence means that the assignments given must be regarded as tentative. The disagreement between the predicted upfield chemical shift for C60-G23 (12.2 or 12.6 ppm) and its assignments to $\epsilon 1$ or $\epsilon 2$ (13.3 ppm) is not regarded as significant, because the neighbors of this base pair are two nonstandard base pairs, whose influences on the chemical shifts of neighboring imino protons were not taken into account in the derivation of the ring current shift rules.

Evidence for Conformational Flexibility. The assignments suggested by the chemical shift rules gain some support from

the behavior of the spectrum of fragment 2 when perturbed by changes in temperature or Mg^{2+} concentration. The thermally sensitive resonances α and β and, at low Mg^{2+} concentration, δ and $\theta 1$ are all assigned nearest the base pairing irregularity which separates helix II from helix III. The fact that the melting of all these resonances, even in low Mg^{2+} concentration, is reversible is consistent with the assignment of the thermally stable resonances (γ and ζ, $\kappa 2$, λ, $\epsilon 1$, 2,3, and J2) to the helices on the ends of fragment 2, where they serve to hold the strands together under conditions destabilizing to the central region. Should the strands come apart, as they do at room temperature in EDTA solution, renaturation is difficult to achieve.

Raising the temperature does not simply lead to the progressive loss of resonances as the structure melts. The marked decrease in line width and increase in intensity of resonances ζ and $\eta 1$ and $\eta 2$ are evidence for a change to a new conformation.

Relationship of Fragment 2 and 5S RNA. While the spectrum of fragment 2 accounts for many of the features in the spectrum of intact 5S RNA not found in the spectrum of fragment 1, there are some features it fails to account for [e.g., the resonance(s) between resonances E and F; see Figure 10]. This fact is not unexpected. The spectrum of 5S RNA should include resonances corresponding to the helix II base pairs which are missing in fragment 2 (G16-C68, C17-G67), and G18-U65, which is included in the sequence of fragment 2 but is not observed due to its position at the end of helix II. Resonances due to tertiary interactions between the two domains might also be present in the spectrum of whole 5S RNA but would not be found in the spectra of the two fragments. The broad feature at 14.15 ppm in the whole 5S RNA spectrum may reflect a tertiary interaction or alternatively it may correspond to the secondary structure resonance seen at low temperature in the spectrum of fragment 2 downfield of resonance α.

NOE studies of intact 5S RNA have provided evidence for a few NOEs in addition to those due to structures found in fragment 1 (Kime & Moore, 1983b). These nonfragment 1 NOEs correspond to NOEs observed in fragment 2. Strong NOEs were reported by Kime and Moore between resonances in 5S RNA having the same chemical shifts as $\kappa 2$ and λ in fragment 2 and were attributed by them to a GU base pair in helix 2 (G18-U65 or G61-U22). Morever, they observed an NOE between this GU and a GC at 13.30 ppm, and between that GC and another at 12.30 ppm. (These findings were confirmed in part by experiments carried out on the 5S RNA sample whose spectrum appears in Figure 10.) The resonance relating to $\kappa 2$ and λ by NOE in native 5S RNA corresponds in chemical shift to ϵ, and the further NOE onto a GC at 12.3 ppm in native 5S RNA corresponds to what would be expected for an ϵ to θ NOE in fragment 2. Thus, the correspondence in chemical shift between resonances in the spectrum of fragment 2 and features in the spectrum of intact 5S RNA are more than coincidental. The fact that both fragment 1 (Kime & Moore, 1983a) and fragment 2 display NMR spectra whose properties are fully consistent with the three-stem secondary structure model for 5S RNA is strong physical evidence in favor of this now widely accepted model. NMR studies of nuclease-resistant fragments of wheat germ 5S RNA that include the helix II–helix III region likewise have produced support for the three-stem model (A. G. Marshall, unpublished results).

According to the assignment scheme presented here, resonance α provides a key marker for conformation 1 in fragment 2. Under conditions where it disappears, the molecule assumes a different conformation; it is likely that this is conformation 2 as shown in Figure 1. Because a resonance at the chemical shift position corresponding to α is seen in intact 5S RNA in high [Mg^{2+}], we suggest that the helix II–helix III region in the intact molecule also exists in conformation 1 under these conditions. The 5S RNA resonance corresponding to α in fragment 2 is also sensitive to [Mg^{2+}] and subject to early melting. It is significant that this resonance melts at a lower temperature and over a narrower temperature range in whole 5S RNA than does resonance α in fragment 2, suggesting that the switch to another conformation, possibly conformation 2, is easier to achieve in the intact molecule than in fragment 2.

The NMR evidence indicates that helix II should be extended in fragment 2 to include G24 base paired to A59 and U25 base paired to A58. Unfortunately, resonances δ (assigned to U25) and $\theta 1$ (assigned to G24) in fragment 2 are not resolvable in the spectrum of whole 5S RNA. Thus, there is no direct evidence for the existence of these base pairs in whole 5S RNA, but given the good correspondence of other fragment 2 resonances, including resonances α, ι, κ, and λ, to features in the spectrum of intact 5S RNA, there is no reason to assume that the extension of helix 2 should not also exist in 5S RNA. Although it is likely that these bases are paired in the free 5S RNA, it is unlikely that this structure has a functional role when 5S RNA is embedded in the ribosome. The consensus secondary structure derived phylogenetically indicates no base pairing in these positions (Erdmann et al., 1985).

Peculiarities of the Imino Spectrum of Fragment 2. Even the best resolved spectra which we have obtained for fragment 2 display broader lines than expected for a molecule of this size. Moreover, a number of resonances exhibit nonstoichiometric intensities. A number of factors may be contributing to produce these effects. First, our samples are not homogeneous. In roughly 10% of the molecules, the 5′ strand begins at G18 rather than A15. Also, roughly 5% of the molecules are religated in the loop (C35 or C36 linked to G44), which may result in stabilization of the terminal base pairs of helix III (G33-C49 and A34-U48). These heterogeneities are expected to have little effect on the imino spectrum, however. More significant is the presence of single-stranded tails at the 5′ ends of both strands of fragment 2, which are likely to increase transient intermolecular associations, particularly at the high concentrations used in NMR. Lowering of the Mg^{2+} concentration is expected to discourage aggregation and does in fact improve the line widths.

Finally, if fragment 2 is involved in a dynamic equilibrium between (at least) two conformations, "irregular" spectral features are to be expected. Protons exchanging between two conformations at a rate comparable to the difference in chemical shift of the two environments (intermediate exchange) are expected to display two or more broad, nonstoichiometric resonances (Jardetzky & Roberts, 1981). One mechanism for conformational change in this part of 5S RNA is bulged base migration, involving C26-C28 and G56 in conformation 1 or A57-A59 and U25 in conformation 2. In these positions in the structure, there are several bases on one strand able to pair with a single base on the other. The present understanding of base stacking leads one to favor the pairing of G56 and C28, but the possibility of base pair migration cannot presently be excluded. Bulged base migration would

be expected to occur on a time scale comparable to base pair opening. Base pair lifetimes for AU's and GU's within stable helices are in the range 1–10 ms at 303 K (Leroy et al., 1985; N. B. Leontis and P. B. Moore, unpublished results). GC lifetimes in stable helices are generally greater than 20 ms; however, little is known about lifetimes in molecules with bulged bases, either in DNA or in RNA. Lifetimes of 1–10 ms result in intermediate exchange effects for exchange between environments differing in chemical shifts by 0.9–0.09 ppm at 500 MHz (Jardetzky & Roberts, 1981). Slow exchange effects occur for larger chemical shift differences and fast exchange for smaller differences. The chemical shifts expected for the bulge migrations under consideration are all less than 1 ppm. Thus, if bulged base migration is occurring, it is likely to produced broad, nonstoichiometric resonances characteristic of intermediate exchange. Possible candidates include resonances ι, which splits into two resonances at low temperature or low Mg^{2+} concentration (Figure 8), and the resonances between about 12.5 and 13.0 ppm. The switch between conformations 1 and 2, on the other hand, involves breaking and remaking several base pairings and is therefore expected to occur on a slower time scale and give rise to effects characteristic of slow exchange.

Comparison with Nuclease Sensitivity Studies. Numerous studies have been reported in which the secondary and tertiary structure of 5S RNA has been probed with chemical and enzymatic agents. Douthwaite and Garret (1981) have shown that the helix II–helix III region of intact 5S RNA is largely resistant to the single-strand-specific ribonucleases A, T1, and T2, when probed in high Mg^{2+} buffer (30 mM Tris, pH 7.8, 20 mM $MgCl_2$, and 300 mM KCl). Under these conditions, the RNA is in the A_H form (native A conformation, high $[Mg^{2+}]$; Kao & Crothers, 1980; Kime & Moore, 1982). They found primary cuts occur only at A52 (RNase T2) and at U65. In recent work, the same group has probed the native state of 5S RNA in low $[Mg^{2+}]$ (the "A_L" form) with the same single-strand-specific RNases (Christensen et al., 1985). Their experiments were conducted at 273 K in low $[Mg^{2+}]$ (40 mM Tris, pH 7.5, 0.5 mM $MgCl_2$, and 30 mM KCl). They found a new primary RNase T1 cut in the A_L form at residue A29, in addition to the primary cut at A52, which occurs in both the A_L and A_H forms. They concluded that this provides evidence for the conformational switch proposed by De Wachter, reasoning that the A_H form corresponds to conformation 1, in which A29 is base paired and therefore protected, whereas the A_L form corresponds to conformation 2, in which A29 is no longer base paired and therefore sensitive to the nuclease. This agrees with our conclusion that under "native" (high $[Mg^{2+}]$) conditions, fragment 2 is in conformation 1 but that low $[Mg^{2+}]$ favors conformation 2. At 0.5 mM Mg^{2+} (pH 7.2, 100 mM KCl), we observe resonance α in whole 5S RNA at 283 K or below. However, as mentioned above, the transition to conformation 2, as reported by the melting of resonance α, occurs by 293 K in whole 5S RNA, at substantially lower temperature than in fragment 2. Moreover, only a small fraction of the molecules need to be present in the nuclease-sensitive A_L form for reaction to occur at a detectable rate. In short, the NMR data on fragment 2 lead to the same conclusions regarding the conformational flexibility of this part of 5S RNA as do the nuclease sensitivity results of Christiansen et al.

ACKNOWLEDGMENTS

We thank Grace Sun and Betty Rennie Freeborn for able technical assistance in sample preparation and Peter Demou of the Yale Chemical Instrumentation Center for facilitating the NMR experiments.

Registry No. RNase, 9001-99-4; Mg, 7439-95-4.

REFERENCES

Brosius, J. (1984) *Gene 27*, 161–172.

Chang, L.-H., Li, S.-J., & Marshall, A. G. (1985) in *Book of Abstracts, Fourth Conversation in Biomolecular Stereodynamics*, June 4–8, 1985 (Ramaswamy, H. S., Ed.), pp 252–253, Institute of Biomolecular Stereodynamics, Albany, NY.

Chou, S.-H., Wemmer, D. E., Hare, D. R., & Reid, B. R. (1984) *Biochemistry 23*, 2257–2262.

Christensen, A., Mathiesen, M., Peattie, D., & Garrett, R. A. (1985) *Biochemistry 24*, 2284–2291.

Christiansen, J., Douthwaite, S. R., Christensen, A., & Garrett, R. A. (1985) *EMBO J. 4*, 1019–1024.

Delihas, N., Andersen, J. & Singhal, R. P. (1984) *Prog. Nucleic Acid Res. Mol. Biol. 31*, 161–190.

De Wachter, R., Chen, M.-W., & Vandenberghe, A. (1982) *Biochimie 64*, 311–329.

De Wachter R., Chen, M.-W., & Vandenberghe, A. (1984) *Eur. J. Biochem. 143*, 175–182.

Donis-Keller, H., Maxam, A. M., & Gilbert, W. (1977) *Nucleic Acids Res. 4*, 2527–2538.

Douthwaite, S., & Garrett, R. A. (1981) *Biochemistry 20*, 7301–7307.

Douthwaite, S., Garrett, R. A., Wagner, R., & Feunteun, J. (1979) *Nucleic Acids Res. 6*, 2453–2470.

Douthwaite, S., Christensen, A., & Garrett, R. A. (1982) *Biochemistry 21*, 2313–2320.

Hare, D. R., & Reid, B. R. (1982a) *Biochemistry 21*, 5129–5135.

Hare, D. R., & Reid, B. R. (1982b) *Biochemistry 21*, 1835–1842.

Jardetzky, O., & Roberts, G. C. K. (1981) *NMR in Molecular Biology*, pp 120–122, Academic Press, New York.

Johnston, P. D., & Redfield, A. G. (1977) *Nucleic Acids Res. 4*, 3599–3615.

Johnston, P. D., & Redfield, A. G. (1981) *Biochemistry 20*, 1147–1156.

Kao, T. H., & Crothers, D. M. (1980) *Proc. Natl. Acad. Sci. U.S.A. 77*, 3360–3364.

Kearns, D. R. (1976) *Prog. Nucleic Acid Res. Mol. Biol. 18*, 91–149.

Kearns, D. R., & Shulman, R. G. (1974) *Acc. Chem. Res. 7*, 33–39.

Kime, M. J., & Moore, P. B. (1982) *Nucleic Acids Res. 10*, 4973–4983.

Kime, M. J., & Moore P. B. (1983a) *Biochemistry 22*, 2615–2622.

Kime, M. J., & Moore, P. B. (1983b) *Biochemistry 22*, 2622–2629.

Kime, M. J., Gewirth, D. T., & Moore, P. B. (1984) *Biochemistry 23*, 3559–3568.

Leory, J.-L., Broseta, D., & Gueron, M. (1985) *J. Mol. Biol. 184*, 165–178.

Peattie, D. A., Douthwaite, S., Garrett, R. A., & Noller, H. F. (1981) *Proc. Natl. Acad. Sci. U.S.A. 78*, 7331–7335.

Robillard, G. T. (1977) in *NMR in Biology* (Dwek, R. A., Campbell, I. D., Richards, R. E., & Williams, R. J. P., Eds.) pp 201–230, Academic Press, New York.

Romaniuk, P. J., Hughes, D. W., Gregoire, R. J., Neilson, T., & Bell, R. A. (1979) *J. Chem. Soc., Chem. Commun.*, 559–560.

Roth, K., Kimber, B. J., & Feeney, J. (1980) *J. Magn. Reson. 41*, 302–309.
Roy, S., & Redfield, A. G. (1981) *Nucleic Acids Res. 9*, 7073–7083.
Roy, S., Papastavros, M. Z., & Redfield, A. G. (1982) *Biochemistry 21*, 6081–6088.
Sanchez, V., Redfield, A. G., Johnston, P. D., & Tropp, J. (1980) *Proc. Natl. Acad. Sci. U.S.A. 77*, 5659–5662.

Ficoll and Dextran Enhance Adhesion of Sendai Virus to Liposomes Containing Receptor (Ganglioside G_{D1a})†

Anne M. Haywood* and Bradley P. Boyer‡

Departments of Pediatrics, Medicine, and Microbiology, University of Rochester Medical Center, Rochester, New York 14642

Received December 13, 1985; Revised Manuscript Received March 7, 1986

ABSTRACT: Previous work has shown that high-speed centrifugation (300000*g*) of Sendai virus and liposomes in 40% (w/v) sucrose layered under a discontinuous *sucrose* gradient removes Sendai virus bound to liposomes containing the ganglioside G_{D1a}, a Sendai virus receptor. Centrifugation also removes virus bound to liposomes containing other negatively charged lipids. This work shows that centrifugation of virus through a discontinuous *ficoll* gradient does not remove virus bound to liposomes containing G_{D1a} but does remove virus from liposomes containing various other negatively charged lipids including the ganglioside G_{M1}, which is not a Sendai virus receptor. The amount of virus that adheres to liposomes increases with increasing content of G_{D1a} in the liposomes. The adhesion of virus to receptor-containing liposomes during centrifugation through a ficoll gradient results from the presence of ficoll and increases with increasing ficoll concentration. Virus also adheres to receptor-containing liposomes during centrifugation in the presence of dextran. These data indicate that caution should be used in interpreting associations demonstrated by centrifugation through dextran and ficoll gradients. They also indicate that binding of virus by ganglioside receptors can be modulated by carbohydrate polymers, which are thought not to have any specific interaction with either viruses or gangliosides.

Sendai viruses bind to liposomes and cells at 0–4 °C but only penetrate them by endocytosis or by membrane fusion at higher temperatures. This fact means that binding can be studied at low temperatures without the complication of concurrent viral membrane fusion. In previous work it has been shown that high-speed centrifugation through a discontinuous sucrose gradient removes Sendai virus from liposomes containing G_{D1a} or other negatively charged lipids (Maeda et al., 1981; Haywood & Boyer, 1982, 1984). Lyles and Landsberger (1979) noted that centrifugation of Sendai virus bound to red cells through a dextran gradient did not remove bound virus. This work was undertaken to resolve the differences between these results. One reason for these differences turned out to be that adhesion of virus to receptors is greater in ficoll or dextran than in sucrose.

Materials and Methods

Virus. Virus was grown and radiolabeled in embryonated eggs, purified, and dialyzed against PBS (137 mM NaCl, 2.7 mM KCl, 8 mM Na_2HPO_4, and 1.5 mM KH_2PO_4) as previously described (Haywood & Boyer, 1982). The protein content of the virus preparation was measured by a modification of the Lowry procedure (Markwell et al., 1978). The virus preparation used in Tables I and II had a specific activity of 1040 cpm/μg of protein. The virus preparation used in Tables III and IV had a specific activity of 132 cpm/μg of protein.

Ficoll, Dextran, and Fetuin. Ficoll 400, M_w 400 000 ± 100 000, and ficoll 70, M_w 68 000 and M_n 25 000, were obtained from Pharmacia Fine Chemicals. Dialyzed ficoll, dextran, M_w 9000, and fetuin, type III lyophilized from fetal calf serum, were obtained from Sigma Chemical Co.

Lipids. Egg phosphatidylcholine (PC), egg phosphatidylethanolamine (PE), egg phosphatidic acid (PA), bovine brain sphingomyelin, bovine brain phosphatidylserine (PS), and bovine brain phosphatidylinositol (PI) were obtained from Avanti Biochemicals. Globoside was obtained from Supelco. Cholesterol, chromatography standard grade, and dicetyl phosphate were obtained from Sigma Chemical Co. When 0.8 μmol of these lipids was chromatographed with chloroform/methanol/concentrated NH_4OH (60:25:4 v/v) and with chloroform/methanol/acetic acid/water (65:25:2:4 v/v) on silica gel G thin-layer chromatography plates, only one spot was observed. Ganglioside G_{D1a} was also obtained from Supelco, Inc. Only one spot was obtained when 0.3 μmol was chromatographed with chloroform/methanol/2.5 M NH_4OH (60:35:8 v/v) plus 20 mg of KCl/100 mL. The concentrations of the phospholipids were determined by the phosphate assay of Ames and Dubin (1960), and the concentration of G_{D1a} was determined by the sialic acid assay of Miettinen and Takki-Luukkainen (1959).

Formation of Liposomes. Multilamellar liposomes were made in PBS as previously described (Haywood & Boyer, 1982). Virus and liposomes were usually combined in 0.3-mL total volume.

Scintillation Counting. Ficoll forms a precipitate in many scintillation fluids. This was initially circumvented by pre-

†This work was supported by National Science Foundation Grant PM-8205896.
‡Present address: American Red Cross, Rochester, NY 14607.

0006-2960/86/0425-3925$01.50/0